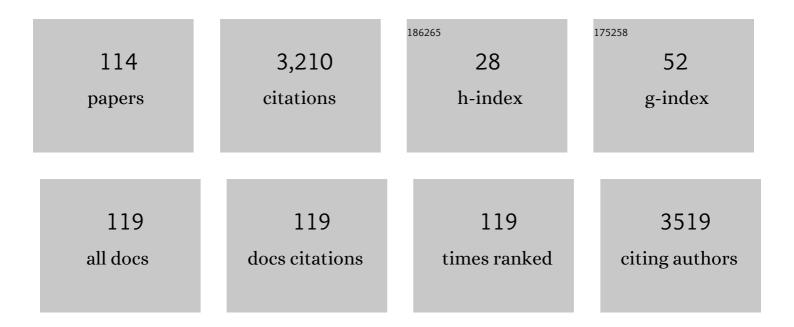
List of Publications by Year in descending order

Source: https://exaly.com/author-pdf/2213250/publications.pdf Version: 2024-02-01



#	Article	IF	CITATIONS
1	High-temperature heat capacity and thermal expansion ofSrTiO3andSrZrO3perovskites. Physical Review B, 1996, 53, 3013-3022.	3.2	301
2	Chairside CAD/CAM materials. Part 1: Measurement of elastic constants and microstructural characterization. Dental Materials, 2017, 33, 84-98.	3.5	287
3	Advances in Raman Spectroscopy Applied to Earth and Material Sciences. Reviews in Mineralogy and Geochemistry, 2014, 78, 509-541.	4.8	135
4	Effect of chemical composition on borosilicate glass behavior under irradiation. Journal of Non-Crystalline Solids, 2010, 356, 388-393.	3.1	117
5	Effect of temperature and thermal history on borosilicate glass structure. Physical Review B, 2012, 85,	3.2	117
6	Boron Speciation in Sodaâ€Lime Borosilicate Glasses Containing Zirconium. Journal of the American Ceramic Society, 2010, 93, 2693-2704.	3.8	111
7	Kinetics and mechanisms of iron redox reactions in silicate melts: The effects of temperature and alkali cations. Geochimica Et Cosmochimica Acta, 2008, 72, 2157-2168.	3.9	105
8	Environments around Al, Si, and Ca in aluminate and aluminosilicate melts by X-ray absorption spectroscopy at high temperature. American Mineralogist, 2008, 93, 228-234.	1.9	86
9	Strain-activated light-induced halide segregation in mixed-halide perovskite solids. Nature Communications, 2020, 11, 6328.	12.8	86
10	Permanent densification of compressed silica glass: a Raman-density calibration curve. Journal of Physics Condensed Matter, 2013, 25, 025402.	1.8	70
11	Development and characterization of lithium-releasing silicate bioactive glasses and their scaffolds for bone repair. Journal of Non-Crystalline Solids, 2016, 432, 65-72.	3.1	63
12	Mapping of rare earth elements in nuclear waste glass–ceramic using micro laser-induced breakdown spectroscopy. Spectrochimica Acta, Part B: Atomic Spectroscopy, 2013, 87, 139-146.	2.9	55
13	Femtosecond laser induced density changes in GeO_2 and SiO_2 glasses: fictive temperature effect [Invited]. Optical Materials Express, 2011, 1, 605.	3.0	53
14	Progressive transformations of silica glass upon densification. Journal of Chemical Physics, 2012, 137, 124505.	3.0	51
15	The crystal and melt structure of spinel and alumina at high temperature: An in-situ XANES study at the Al and Mg K-edge. Geochimica Et Cosmochimica Acta, 2009, 73, 3410-3422.	3.9	45
16	Energetics of kaolin polymorphs. American Mineralogist, 1999, 84, 506-516.	1.9	43
17	Heat capacity and entropy of rutile (TiO 2) and nepheline (NaAlSiO 4). Physics and Chemistry of Minerals, 2002, 29, 267-272.	0.8	40
18	Observation of O_2 inside voids formed in GeO_2 glass by tightly-focused fs-laser pulses. Optical Materials Express, 2011, 1, 1150.	3.0	39

#	Article	IF	CITATIONS
19	Fracture anisotropy in texturized lithium disilicate glass-ceramics. Journal of Non-Crystalline Solids, 2018, 481, 457-469.	3.1	39
20	Elastic anomalous behavior of silica glass under high-pressure: In-situ Raman study. Journal of Non-Crystalline Solids, 2009, 355, 1095-1098.	3.1	38
21	Decoupling of viscosity and relaxation processes in supercooled water: a molecular dynamics study with the TIP4P/2005f model. Physical Chemistry Chemical Physics, 2017, 19, 2124-2130.	2.8	37
22	Effect of thermally induced structural disorder on the chemical durability of International Simple Glass. Npj Materials Degradation, 2018, 2, .	5.8	37
23	Silica under hydrostatic pressure: A non continuous medium behavior. Journal of Non-Crystalline Solids, 2009, 355, 2422-2424.	3.1	34
24	Development and characterization of niobium-releasing silicate bioactive glasses for tissue engineering applications. Journal of the European Ceramic Society, 2018, 38, 871-876.	5.7	33
25	Low-temperature heat capacity of GeO2 and B2O3 glasses: thermophysical and structural implications. Journal of Non-Crystalline Solids, 2003, 315, 20-30.	3.1	32
26	Structural heterogeneity and pressure-relaxation in compressed borosilicate glasses by in situ small angle X-ray scattering. Journal of Chemical Physics, 2011, 134, 204502.	3.0	32
27	Polyamorphic transitions in silica glass. Journal of Non-Crystalline Solids, 2013, 382, 133-136.	3.1	32
28	Relaxation processes of densified silica glass. Journal of Chemical Physics, 2017, 146, .	3.0	30
29	Synthesis and luminescent properties of Eu3+/Eu2+ co-doped calcium aluminosilicate glass–ceramics. Journal of Luminescence, 2016, 169, 528-533.	3.1	29
30	Local densification of a single micron sized silica sphere by uniaxial compression. Scripta Materialia, 2015, 108, 84-87.	5.2	28
31	In situ High-Temperature Experiments. Reviews in Mineralogy and Geochemistry, 2014, 78, 779-800.	4.8	27
32	Spectroscopic study of the role of alkaline earth oxides in mixed borate glasses - site basicity, polarizability and glass structure. Journal of Non-Crystalline Solids, 2020, 533, 119892.	3.1	27
33	Indentation densification of fused silica assessed by raman spectroscopy and constitutive finite element analysis. Journal of the American Ceramic Society, 2020, 103, 3076-3088.	3.8	27
34	Photoreduction of iron by a synchrotron X-ray beam in low iron content soda-lime silicate glasses. Chemical Geology, 2013, 346, 106-112.	3.3	26
35	<i>In situ</i> Brillouin study of sodium alumino silicate glasses under pressure. Journal of Chemical Physics, 2013, 139, 074501.	3.0	26
36	In situ structural changes of amorphous diopside (CaMgSi2O6) up to 20 GPa: A Raman and O K-edge X-ray Raman spectroscopic study. Geochimica Et Cosmochimica Acta, 2016, 178, 41-61.	3.9	26

#	Article	IF	CITATIONS
37	Combined Differential scanning calorimetry, Raman and Brillouin spectroscopies: A multiscale approach for materials investigation. Analytica Chimica Acta, 2018, 998, 37-44.	5.4	26
38	Impact of magnesium on the structure of aluminoborosilicate glasses: A solidâ€state NMR and Raman spectroscopy study. Journal of the American Ceramic Society, 2021, 104, 4518-4536.	3.8	26
39	Silica polymorphs, glass and melt: An in situ high temperature XAS study at the Si K-edge. Journal of Non-Crystalline Solids, 2009, 355, 1099-1102.	3.1	25
40	Emission tunability and local environment in europium-doped OHâ^'-free calcium aluminosilicate glasses for artificial lighting applications. Materials Chemistry and Physics, 2015, 156, 214-219.	4.0	25
41	Entropy of calcium and magnesium aluminosilicate glasses. Chemical Geology, 1996, 128, 113-128.	3.3	24
42	Correlation between boson peak and anomalous elastic behavior in GeO2 glass: An <i>in situ</i> Raman scattering study under high-pressure. Journal of Chemical Physics, 2011, 134, 234503.	3.0	24
43	Cerium/aluminum correlation in aluminosilicate glasses and optical silica fiber preforms. Journal of Non-Crystalline Solids, 2017, 475, 85-95.	3.1	24
44	Thermal and optical properties of binary magnesium tellurite glasses and their link to the glass structure. Journal of Alloys and Compounds, 2020, 823, 153781.	5.5	24
45	Chemical Durability of Lanthanumâ€Enriched Borosilicate Glass. International Journal of Applied Glass Science, 2013, 4, 383-394.	2.0	23
46	Europium-Doped Tellurite Glasses: The Eu2+ Emission in Tellurite, Adjusting Eu2+ and Eu3+ Emissions toward White Light Emission. Materials, 2019, 12, 4140.	2.9	22
47	Behaviour of the Eu3+ 5D0→7F0 transition in CaMoO4 powellite type ceramics under Ar and Pb ions implantation. Optical Materials, 2011, 34, 386-390.	3.6	21
48	Chemical tunability of europium emission in phosphate glasses. Journal of Luminescence, 2017, 183, 53-61.	3.1	20
49	Fluorescence line narrowing and Judd-Ofelt theory analyses of <mml:math xmlns:mml="http://www.w3.org/1998/Math/MathML" altimg="si0042.gif" overflow="scroll"><mml:msup><mml:mrow><mml:mi>Eu</mml:mi></mml:mrow><mml:mrow><mml:mn>3low-silica calcium aluminosilicate glass and glass-ceramic. lournal of Luminescence, 2018, 201, 123-128.</mml:mn></mml:mrow></mml:msup></mml:math 	ıml:mħ> <r< td=""><td>nml:mo>+</td></r<>	nml:mo>+
50	Optical Properties and Bismuth Redox in Bi-Doped High-Silica Al–Si Glasses. Journal of Physical Chemistry C, 2018, 122, 19777-19792.	3.1	19
51	Ca neighbors from XANES spectroscopy: A tool to investigate structure, redox, and nucleation processes in silicate glasses, melts, and crystals. American Mineralogist, 2016, 101, 1232-1235.	1.9	18
52	The structure of haplobasaltic glasses investigated using X-ray absorption near edge structure (XANES) spectroscopy at the Si, Al, Mg, and O K -edges and Ca, Si, and Al L 2,3 -edges. Chemical Geology, 2016, 420, 213-230.	3.3	18
53	Influence of Vanadium on Optical and Mechanical Properties of Aluminosilicate Glasses. Frontiers in Materials, 2020, 7, .	2.4	17
54	Experimental study of dissolution rates of hedenbergitic clinopyroxene at high temperatures: dissolution in water from 25 °C to 374 °C. European Journal of Mineralogy, 2013, 25, 353-372.	1.3	16

#	Article	IF	CITATIONS
55	Phase Transformation in Laserâ€Induced Microâ€Explosion in Olivine (Fe,Mg) ₂ SiO ₄ . Advanced Engineering Materials, 2014, 16, 767-773.	3.5	16
56	Cooling rate calibration and mapping of ultra-short pulsed laser modifications in fused silica by Raman and Brillouin spectroscopy. International Journal of Extreme Manufacturing, 2020, 2, 035001.	12.7	16
57	Nucleation mechanisms in a SiO2-Li2O-P2O5-ZrO2 biomedical glass-ceramic: Insights on crystallisation, residual glasses and Zr4+ structural environment. Journal of the European Ceramic Society, 2022, 42, 1762-1775.	5.7	16
58	Behaviour of simplified nuclear waste glasses under gold ions implantation: A microluminescence study. Journal of Nuclear Materials, 2007, 362, 480-484.	2.7	15
59	Dynamics of iron-bearing borosilicate melts: Effects of melt structure and composition on viscosity, electrical conductivity and kinetics of redox reactions. Journal of Non-Crystalline Solids, 2013, 373-374, 18-27.	3.1	15
60	Irradiated rareâ€earthâ€doped powellite single crystal probed by confocal Raman mapping and transmission electron microscopy. Journal of Raman Spectroscopy, 2014, 45, 383-391.	2.5	15
61	<i>In situ</i> structural analysis of calcium aluminosilicate glasses under high pressure. Journal of Physics Condensed Matter, 2016, 28, 315402.	1.8	15
62	Low-temperature degradation increases the cyclic fatigue resistance of 3Y-TZP in bending. Dental Materials, 2020, 36, 1086-1095.	3.5	15
63	Evidence of polyamorphic transitions during densified SiO2 glass annealing. Journal of Chemical Physics, 2019, 151, 164502.	3.0	14
64	Shape-anisotropic cobalt-germanium-borate glass flakes as novel Li-ion battery anodes. Powder Technology, 2020, 363, 218-231.	4.2	14
65	Influence of Al2O3 Addition on Structure and Mechanical Properties of Borosilicate Classes. Frontiers in Materials, 2020, 7, .	2.4	14
66	Raman Spectroscopy of Adsorbed Water in Clays: First Attempt at Band Assignment. Procedia Earth and Planetary Science, 2013, 7, 203-206.	0.6	13
67	Luminescent properties of Eu-doped calcium aluminosilicate glass-ceramics: A potential tunable luminophore. Optical Materials, 2018, 85, 41-47.	3.6	13
68	Cerium speciation in silicate glasses: Structure-property relationships. Journal of Non-Crystalline Solids, 2021, 563, 120785.	3.1	13
69	Effects of Medium pH and Preconditioning Treatment on Protein Adsorption on 45S5 Bioactive Glass Surfaces. Advanced Materials Interfaces, 2020, 7, 2000420.	3.7	12
70	Determining the local pressure during aerosol deposition using glass memory. Journal of the American Ceramic Society, 2020, 103, 2443-2452.	3.8	11
71	Tailoring the Mechanical Properties of Metaluminous Aluminosilicate Glasses by Phosphate Incorporation. Frontiers in Materials, 2020, 7, .	2.4	11
72	Colors in Glasses. Springer Handbooks, 2019, , 297-342.	0.6	11

#	Article	IF	CITATIONS
73	Kinetics of iron redox reaction in silicate melts: A high temperature Xanes study on an alkali basalt. Journal of Physics: Conference Series, 2009, 190, 012182.	0.4	10
74	Laser-induced structural changes in pure GeO2 glasses. Journal of Non-Crystalline Solids, 2011, 357, 2637-2640.	3.1	10
75	Low-frequency Raman scattering under high pressure in diamond anvil cell: Experimental protocol and application to GeO2 and SiO2 boson peaks. Journal of Non-Crystalline Solids, 2012, 358, 3156-3160.	3.1	10
76	Assessment of elastic models in supercooled water: A molecular dynamics study with the TIP4P/2005f force field. Journal of Chemical Physics, 2017, 147, 014504.	3.0	10
77	Bioactive glass coating using aerosol deposition. Ceramics International, 2019, 45, 14728-14732.	4.8	10
78	Structure—longitudinal sound velocity relationships in glassy anorthite (CaAl2Si2O8) up to 20 GPa: An in situ Raman and Brillouin spectroscopy study. Geochimica Et Cosmochimica Acta, 2019, 261, 132-144.	3.9	9
79	Development of magnesiumâ€aluminumâ€silicate glassâ€ceramics nucleated with Nb 2 O 5. International Journal of Applied Glass Science, 2020, 11, 155-169.	2.0	9
80	Raman and fluorescence. , 0, , 61-82.		9
81	Contribution of neodymium optical spectroscopy to the crystal growth study of a silicate apatite in a glassy matrix. Optical Materials, 2008, 30, 1694-1698.	3.6	8
82	In situ combined stress―and temperatureâ€dependent Raman spectroscopy of Liâ€doped (Na,K)NbO ₃ . Journal of the American Ceramic Society, 2022, 105, 2735-2743.	3.8	8
83	Luminescent centres in pezzottaite, CsBe2LiAl2Si6O18. European Journal of Mineralogy, 2010, 22, 605-612.	1.3	7
84	Wet-chemical porosification of LTCC substrates: Dissolution mechanism and mechanical properties. Microporous and Mesoporous Materials, 2019, 288, 109593.	4.4	7
85	Thermal Evolutions to Glass-Ceramics Bearing Calcium Tungstate Crystals in Borate Glasses Doped with Photoluminescent Eu3+ Ions. Materials, 2021, 14, 952.	2.9	7
86	Enhanced Electromechanical Response and Thermal Stability of 0.93(Na _{1/2} Bi _{1/2})TiO ₃ â€0.07BaTiO ₃ Through Aerosol Deposition of Base Metal Electrodes. Advanced Materials Interfaces, 2021, 8, 2100309.	3.7	7
87	Devitrification Behavior of Sol-Gel Derived ZrO2-SiO2 Rare-Earth Doped Glasses: Correlation between Structural and Optical Properties. Ceramics, 2018, 1, 274-286.	2.6	6
88	Simulation of Eu3+ luminescence spectra of borosilicate glasses by molecular dynamics calculations. Optical Materials, 2008, 30, 1689-1693.	3.6	5
89	Pressure-independent Brillouin Fiber Optic Sensors for temperature measurements. Journal of Non-Crystalline Solids, 2014, 401, 36-39.	3.1	5
90	Correlation between mechanical and structural properties as a function of temperature within the TeO2–TiO2–ZnO ternary system. Journal of Non-Crystalline Solids, 2020, 528, 119716.	3.1	5

#	Article	IF	CITATIONS
91	Relaxation behavior of densified sodium aluminoborate glass. Acta Materialia, 2020, 198, 153-167.	7.9	5
92	The influence of codoping on optical properties and glass connectivity of silica fiber preforms. Ceramics International, 2020, 46, 26251-26259.	4.8	5
93	Surface Probing of Ultraâ€Shortâ€Pulse Laser Filament Cut Window Glass and the Impact on the Separation Behavior. Advanced Engineering Materials, 2020, 22, 2000471.	3.5	4
94	Coupling Raman, Brillouin and Nd3+ Photo Luminescence Spectroscopy to Distinguish the Effect of Uniaxial Stress from Cooling Rate on Soda–Lime Silicate Glass. Materials, 2021, 14, 3584.	2.9	4
95	Ultra-Short-Pulse Laser Filaments for Float Glass Cutting: Influence of Laser Parameters on Micro Cracks Formation. Frontiers in Physics, 2022, 10, .	2.1	4
96	Investigation of Aluminate and Al2O3 Crystals and Melts at High Temperature Using XANES Spectroscopy. AlP Conference Proceedings, 2007, , .	0.4	3
97	On the induction of homogeneous bulk crystallization in Eu-doped calcium aluminosilicate glass by applying simultaneous high pressure and temperature. Journal of Applied Physics, 2016, 119, 245901.	2.5	3
98	Analysis of shockwave formation in glass welding by ultra-short pulses. Procedia CIRP, 2018, 74, 339-343.	1.9	3
99	Modeling the effect of the addition of alumina on structural characteristics and tensile deformation response of aluminosilicate glasses. Ceramics International, 2020, 46, 21657-21666.	4.8	3
100	Eu3+-doped lithium tellurite glasses prepared under vacuum condition: Spectroscopic investigation and energy transfer mechanism. Journal of Luminescence, 2022, 246, 118812.	3.1	3
101	Iron Redox Reactions in Model Nuclear Waste Glasses and Melts. Materials Research Society Symposia Proceedings, 2008, 1124, 1.	0.1	2
102	Structure of spinel at high temperature using <i>in-situ</i> XANES study at the Al and Mg K-edge. Journal of Physics: Conference Series, 2009, 190, 012178.	0.4	2
103	Permanent Ge Coordination Change Induced by Pressure in La ₂ O ₃ –B ₂ O ₃ –GeO ₂ Glass. Journal of the American Ceramic Society, 2010, 93, 2726-2730.	3.8	2
104	13. Advances in Raman Spectroscopy Applied to Earth and Material Sciences. , 2014, , 509-542.		2
105	Progress and challenges in advanced ground-based gravitational-wave detectors. General Relativity and Gravitation, 2014, 46, 1.	2.0	2
106	Utilizing Rare-Earth-Elements Luminescence and Vibrational-Spectroscopies to Follow High Pressure Densification of Soda–Lime Glass. Materials, 2021, 14, 1831.	2.9	2
107	Room temperature deposition of freestanding BaTiO3 films: temperature-induced irreversible structural and chemical relaxation. Journal of Materials Science, 2022, 57, 13264-13286.	3.7	2
108	An In Situ High Temperature Investigation of Cation Environments in Aluminate and Silicate Glasses and Liquids at the LUCIA Beamline. AIP Conference Proceedings, 2007, , .	0.4	1

#	Article	IF	CITATIONS
109	Structural and optical characterization of crystals obtained via solid state reactions in the In2O3–TiO2–Al2O3 pseudoternary system. SN Applied Sciences, 2019, 1, 1.	2.9	1
110	The Silicon Environment in Silica Polymorphs, Aluminosilicate Crystals and Melts: An In Situ High Temperature XAS Study. AIP Conference Proceedings, 2007, , .	0.4	0
111	19. In situ High-Temperature Experiments. , 2014, , 779-802.		0
112	Melting Curves of Triolein Polymorphs. JAOCS, Journal of the American Oil Chemists' Society, 2021, 98, 211-219.	1.9	0
113	Glass Machining and In-situ Metrology: recovery of spatio-temporal phase distribution from 2-dimensional interference fringe movement caused by irradiation of glass with ultra-short laser pulses at high pulse repetition rates. , 2019, , .		0
114	Glass formation, physical and structural investigation studies of the (90-x) Sb2O3-10WO3-xNaPO3 glasses. Materials Today Communications, 2022, 30, 103226.	1.9	0